Fatigue behaviour of threaded rods bonded into glued-laminated timber for application in bridge construction

René Steiger, Empa – Swiss Federal Laboratories for Materials Science and Technology, Structural Engineering Research Laboratory, Dübendorf, Switzerland

Bruno Zumbrunn-Maurer, neue Holzbau AG, Lungern, Switzerland

Lukas Kramer, Empa – Swiss Federal Laboratories for Materials Science and Technology, Structural Engineering Research Laboratory, Dübendorf, Switzerland

Thomas Strahm, neue Holzbau AG, Lungern, Switzerland

Ernst Gehri, Prof. em. ETH Zürich, Dr. h. c., Rüschlikon Switzerland

Keywords: Fatigue strength, stiffness, road bridges, bonded-in threaded steel rods, Service Class 1 / 2 / 3

1 Introduction

Due to their high load-carrying capacity (resistance) and stiffness, corrosion and fire resistance as well as aesthetic advantages, connections with bonded-in threaded or ribbed steel rods (BiR) are frequently used in building construction, for example, for column anchoring, rigid connections, trusses (*Tlustochowicz et al.,* 2010) and reinforcements of various kinds (*Steiger et al.,* 2015). This very efficient type of connection can offer its advantages in bridge construction projects as well. However, timber is still used comparatively little as a building material in bridge construction, in particular for road bridges. Reasons for this are the fatigue stresses caused by traffic loads and the more difficult climatic conditions compared to the construction of buildings.

Current knowledge of the fatigue behaviour of members and connections in timber bases primarily on studies performed with metallic materials (steel, aluminium) that have been adapted for the design of timber structures. The provisions on fatigue design of timber structures in the currently still valid version of Eurocode 5-2 (*CEN,* 2004) were primarily developed for the design of structural members and they only cover selected fastener types such as nails and dowels. Despite the fatigue behaviour of BiR had been investigated, see e.g. (*Bengtsson and Johansson,* 2002), respective normative specifications for the design had been lacking in the first generation

Eurocode 5-2. In the past years, additional investigations on the fatigue resistance of BiR connections were performed (*Bletz-Mühldorfer et al.,* 2018; *Erchinger and Steurer,* 2005; *Maurer et al.,* 2022; *Molina et al.,* 2009; *Myslicki et al.,* 2019; *Myslicki et al.,* 2019); and in the Formal Vote (FV) Draft of FprEN 1995-1-1 (*CEN,* 2025), values representing the type of fatigue effect in the fatigue verification, are specified for axially loaded BiR (a_{fat} = 6.7 and β_{fat} = 1.3).

Connections with BiR are of particular interest for structures with fatigue loading, because they allow a very uniform force transfer when arranged appropriately (*Gehri,* 2000). The absence of stress peaks is generally regarded as the key to get high fatigue strength. So far, most of the experiments on fatigue strength have been carried out on connections in dry wood, i.e. in Service Class SC 1 (*CEN,* 2004)). Transferability to applications in bridge construction, where elevated moisture contents (SC 2 / SC 3) prevail, is limited. Elevated moisture content (MC or ω) significantly affects the mechanical properties of wood. This can impair the resistance, could possibly change the failure mode and reduce the fatigue strength of connections.

A research project recently conducted at Empa in collaboration with the company neue Holzbau AG (n'H) was dedicated to the determination of the fatigue strength of connections with profiled rods bonded into glulam under practical conditions with a focus on bridge construction by taking an elevated MC into account. Examples of such applications are shown in Figure 1.

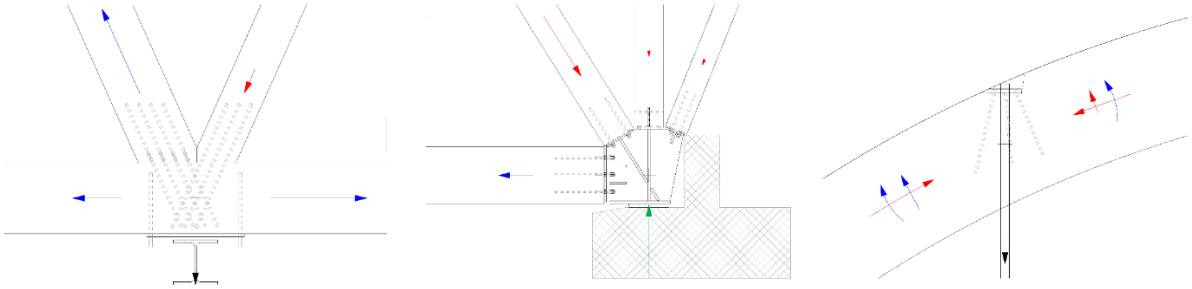

a) b) c)

Figure 1. Examples of application of BiR in bridge construction: Connections timber-to-timber (a) and steel-to-timber (b) in trusses; connections of hangers to arches (c).

2 Methodology and materials

2.1 General approach

The project focused on two configurations of BiR in relation to the grain direction of the timber (parallel ∥ and perpendicular ⊥). Fatigue tests were carried out and the mechanical properties (connection stiffness and resistance under axial tensile force) before and after passing the fatigue test in combination with the influences of the MC were investigated. In addition, the load-bearing behaviour and failure modes were compared with tests on connections subjected to static loading. Four groups of specimens (A – D) with varying type of loading and MC were subjected to testing, according to Table 1.

Table 1. Overview of the tests performed.

Group	Series	Setting of rods vs. grain direction / MC / Type of experiment	Species (GLT)
A	A1	BiR ‖ / Dry wood / Fatigue [1)]	European ash (*Fraxinus excelsior*)
	A2	BiR ‖ / Elevated MC / Static	
	A3	BiR ‖ / Elevated MC / Fatigue + Residual strength static	
B		Optimisation of test set up BiR ⊥ / Dry wood / Static	Norway spruce (*Picea abies*)
C	C1	BiR ⊥ / Dry wood / Static	Norway spruce (*Picea abies*)
	C2	BiR ⊥ / Dry wood / Fatigue + Residual strength static	
D	D1	BiR ⊥ / Elevated MC / Static	Norway spruce (*Picea abies*)
	D2	BiR ⊥ / Elevated MC / Fatigue + Residual strength static	

[1)] Test series A1 had been investigated in the course of an earlier project (*Maurer et al.,* 2022).

2.2 Shape and geometrical properties of the specimens

While it was known from previous experiments (*Maurer et al.,* 2022) that the test setup worked for the fatigue tests on BiR inserted ‖ to grain, a suitable setup first had to be developed for the tests on BiR inserted ⊥ to grain. Figure 2 and Figure 3 show the experimentally examined specimens for the series of BiR ‖ or ⊥ to grain, respectively. For the specimens with BiR ‖ to grain, hardwood was chosen because high forces can be applied here. Compared to softwood, this leads to higher stresses in the bond line. The specimens with BiR ⊥ to grain were designed with two groups of BiR (top 3 GSA in 1 row and bottom 4 GSA in 2 rows) in a way that failure in rolling shear was to be expected. In this mode, which is typical for the nodes of BiR trusses, the failure occurs in the wood between two rows of BiR crossing in the chord (see Figure 1a). Therefore, softwood glulam was chosen to allow for exploring the lower strength limit for this failure mode.

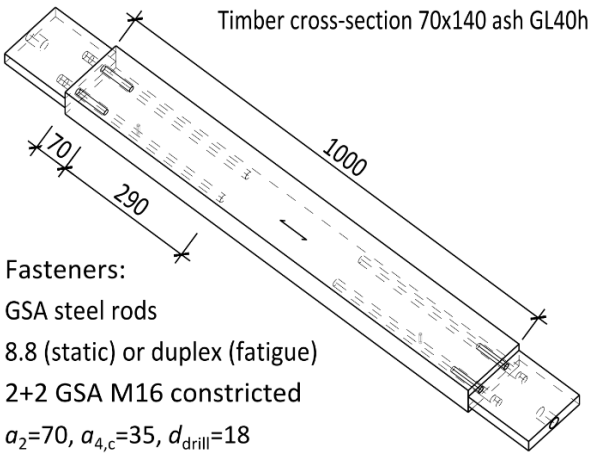

Figure 2. Specimen with 2 pairs of BiR on both sides for fatigue tests ‖ to grain in European ash glulam. All dimensions in [mm].

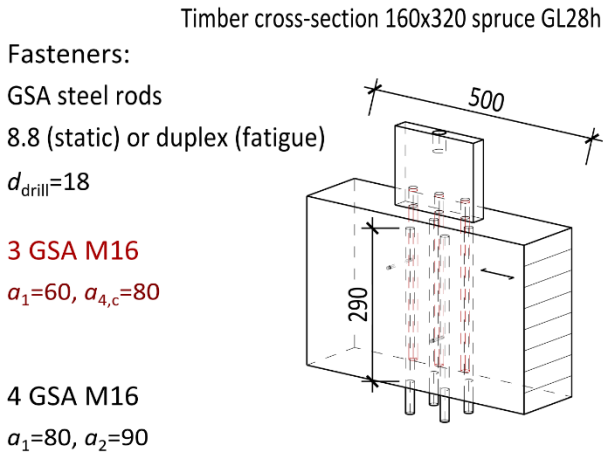

Figure 3. Specimen with 2 groups of BiR for fatigue tests ⊥ to grain in Norway spruce glulam. All dimensions in [mm].

2.3 Materials

2.3.1 Glued-laminated timber (GLT)

Glued-laminated timber (GLT) produced from the most relevant wood species (European ash, *Fraxinus excelsior*, and Norway spruce, *Picea abies*) regarding truss structures in timber dedicated to road bridge construction in Switzerland was chosen. To keep the variations of mechanical properties low, the laminations used for the GLT production were strength graded with the Timber Grader MTG (Brookhuis) into the respective T classes i.e. T18 for Norway spruce and T33 for European ash (*Arnold et al.,* 2021; *Bernasconi et al.,* 2021; *CEN,* 2016). Finally, laminations of uniform densities (groups of laminations with minimized CoV of the density) were selected.

For the series with elevated MC, conditioning of the specimens to an MC of around 20 % was essential for simulating real conditions such as those that occur in bridge structures. Hence, for the series A2, A3, D1 and D2, the laminations used to produce the GLT were stored in an environment with strongly elevated humidity of the surrounding air. A special climate box with water-tight sealing on the inside was developed, and the laminations were stored in that box above a saturated salt-water solution. After first trials with sodium chloride (NaCl), potassium chloride (KCl) was finally used to increase water uptake. The air in the box was ventilated by means of two fans. The MC achieved in the laminations was monitored by weighing them in regular intervals. After the glulam production, joinery and bonding of the rods, the climate boxes were used for further conditioning, storing and transporting the specimens ready for testing. The MC developing in the specimens was monitored indirectly by weighing reference specimens (spruce and ash members with cross-sections between 70 x 70 mm^2 and 160 x 160 mm^2), see Figure 4. The end faces of these four groups of specimens and of all reference specimens were sealed. Two layers of end grain protection from Koch & Schulte were applied with a brush.

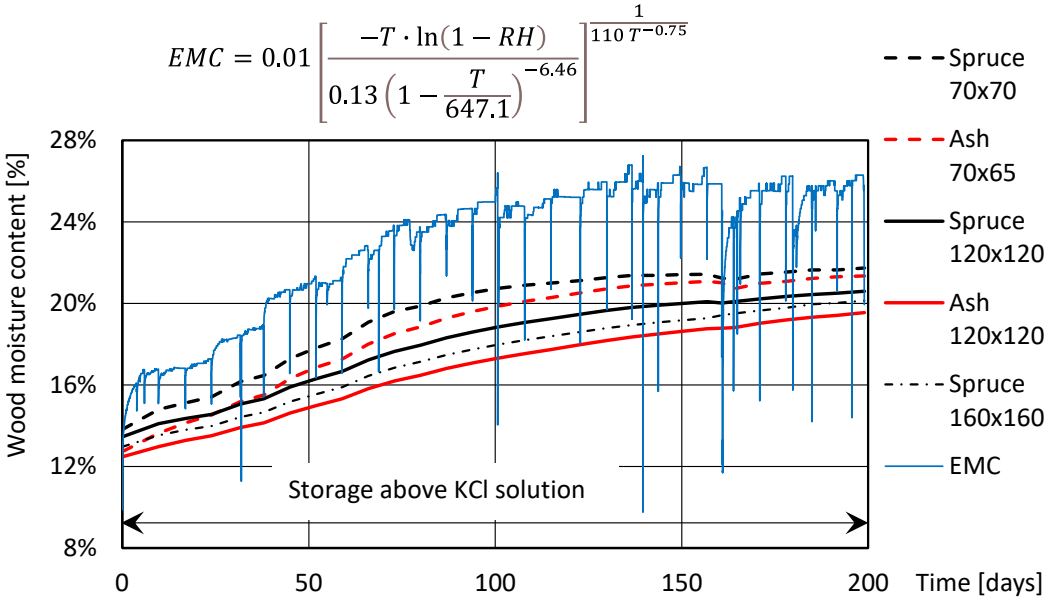

Figure 4. Development of the MC of the reference specimens (calculated equilibrium moisture content (EMC) based on the measured climate in the boxes).

The equilibrium moisture content (EMC) was calculated from the temperature *T* [K] and the relative humidity *RH* [-] according to the formula in Figure 4 (*Reichel,* 2015). The difference between this EMC model and the measured MC of the reference specimens is attributed to the size of the cross-sections. For the GLT properties determined from the tested specimens, the mean values per series are listed below, i.e. density (Table 2, Table 6) and modulus of elasticity MOE (Table 4). The individual values for each specimen are given in (*Steiger and Zumbrunn-Maurer,* 2024). The differences in MOE and density between Series A1 and A2 – A3 result from having chosen raw material from different sawmills.

Table 2. Local densities [kg/m³] at ω = 12 % of the European ash GLT specimens of group A.

Specimen	Series A1	Series A2	Series A3
Mean values	718 [1)]	644	640
		Mean value of group A	662
		CoV of group A	6 %

[1)] Test series A1 had been investigated in the course of an earlier project (*Maurer et al.,* 2022).

Table 3. Bulk densities [kg/m³] at ω = 12 % of the Norway spruce GLT specimens of groups B, C, D.

Specimen	Group B and Series C1	Series C2	Series D1	Series D2
Mean values	429	445	423	424
		Mean value of groups B, C and D		430
		CoV of groups B, C and D		4 %

Table 4. Modulus of elasticity [N/mm²] of the European ash GLT specimens of group A.

Specimen	Series A1	Series A2	Series A3		
Test name [1)]	Proof loading	Pull-out test	Proof loading	Preloading	Pull-out test
MC	≈ 9 %	≈ 20 %	≈ 20 %	≈ 20 %	≈ 17 %
Mean	15'500	11'900	11'300	11'500	11'900

[1)] The names of the static load tests are explained in 2.6.

2.3.2 Bonded-in rod connections

The tested BiR connections were of type GSA (*EOTA,* 2020), consisting of steel rods with metric thread M16 bonded into 18 mm diameter holes by means of a 2-component epoxy resin. The performance of this system is well above the minimum characteristic withdrawal strength according to the FV Draft of FprEN 1995-1-1 (*CEN,* 2025) of $f_{w,k}$ = 4 N/mm². The GSA adhesive passed tensile creep tests at 60 °C according to EN 17334 (*CEN,* 2021) loaded with a shear stress of 7 N/mm² in the bond line. For the actual specimens, the effective anchoring length (withdrawal length) of the rods was 290 mm (i.e. 16.1·d_{drill}). For group A, a recess (not bonded length) of 70 mm was applied. In this part, the thread was removed, and the rod was machined to the appropriate diameter to ensure a ductile failure in the ultimate limit state. With the partial safety factors valid in Switzerland, the design resistance as well as the forces for static proof loading and fatigue testing were calculated (Table 5).

Table 5. Calculated resistances and forces for static proof loading and fatigue testing.

Groups		A	B & C	D
Characteristic value of withdrawal resistance	R_k	200 kN	187 kN	187 kN
Partial safety factor for ductile connections [1)]	γ_M/η_M	1.5	1.5	1.5
Factor considering the influence of the MC [1)]	η_ω	1.0	1.0	0.8
Design value of withdrawal resistance	$R_d = R_k / (\gamma_M/\eta_M)$	133 kN	125 kN	99.8 kN
Conversion factor [2)]	$\gamma_Q + R \cdot \gamma_G$	1.635	1.635	1.635
Assumed variable live load [2)]	Q_k	81.5 kN	73.6 kN	61.0 kN
Chosen level of fatigue loading in tests	ΔF	90.0 kN	81.0 kN	64.8 kN
Force amplitude	F_a	±45 kN	±40.5 kN	±32.4 kN

[1)] according to the Swiss standard SIA 265 for the design of timber structures (*SIA,* 2021).

[2)] The variable live load Q_k is calculated assuming that 90 % of the maximum force acting in the case of fatigue loading (at SLS level) is caused by the fatigue-effective action. This is reflected by the chosen stress ratio R. Based on a maximum utilization in the ULS, the following equation results: $R_d = E_d = 1.35G_k + 1.5Q_k$, which for the chosen case with $G_k/Q_k = R = 0.1$ can be simplified as follows: $Q_k = R_d/1.635$.

The BiR subjected to static loading (series A2, B, C1, D1) were of steel grade 8.8. For the experiments with fatigue loading (series A1, A3, C2, D2), a duplex steel quality was chosen, as investigated in earlier experiments (*Maurer et al.,* 2022).

2.3.3 Steel parts for connecting the specimens with the testing machine

To ensure that no fatigue failure occurred in the steel connecting parts, these had to be developed and optimized regarding the steel quality and the geometric shape prior to the fatigue tests. In series A1 and A3 and for the top joint of the BiR ⊥ to grain series, 30 mm thick steel plates of grade S355J2 were used. The rod-to-plate connection detail corresponded to the design developed in 2021 (*Maurer et al.,* 2022). The other steel parts were fastened by nuts. They were tightened uniformly with a torque of 80 Nm in series A2 and 30 Nm in the bottom joint of the BiR ⊥ to grain series (for details see research report).

2.4 Connection stiffness

For comparing the measured connection stiffnesses with the specifications in the FV Draft of FprEN 1995-1-1 (*CEN,* 2025), Clause 11.3.8.3, the axial slip modulus K_{ax} [kN/mm] is modelled with 3 displacement shares (Equations 1 – 3, below). As an example, for the A2 specimens they result as follows:

Equation 1. Displacement share of the withdrawal length.

$$K_{\mathrm{ax},1} = K_{\mathrm{w}} = 460 \left(\frac{\rho_{\mathrm{mean}}}{420}\right)^{0.85} d^{0.9} {l_{\mathrm{w}}}^{0.6} = \frac{460}{1'000} \cdot \left(\frac{644}{420}\right)^{0.85} \cdot 16^{0.9} \cdot 290^{0.6} = 241$$

Equation 2. Displacement share of the constriction zone.

$$K_{\mathrm{ax},2} = K_{\mathrm{s},1} = \frac{E \cdot A}{l} = \frac{210'000 \cdot 133}{65 \cdot 1'000} = 430$$

Equation 3. Displacement share of the rod length in the steel part incl. washer & nut. (As a simplification for deformations in the threads, the entire length of the nut is considered to be free and fully loaded rod length.)

$$K_{\mathrm{ax,3}} = K_{\mathrm{s,2}} = \frac{E \cdot A}{l} = \frac{210'000 \cdot 157}{74 \cdot 1'000} = 446$$

Equation 4. Slip modulus for the group of 2 GSA M16.

$$K_{\mathrm{ax}} = n \cdot \frac{1}{\sum_{\mathrm{i=1}}^{\mathrm{j}} \frac{1}{K_{\mathrm{ax,i}}}} = 2 \cdot \frac{1}{\frac{1}{241} + \frac{1}{430} + \frac{1}{446}} = 229$$

where d is the diameter of the rod and l_w is the withdrawal length.

2.5 Experiments with fatigue loading

For the main set of experiments, cyclic tests at constant force amplitudes were carried out force-controlled (sinus) in pull-pull configuration (*Tlustochowicz et al.,* 2010) with a stress ratio $R = F_{min}/F_{max} = 0.1$ and frequencies of $f = 4 – 7$ Hz (Table 6). A target value of $N = 2 \cdot 10^6$ stress cycles was defined because the structural steel standards also relate their fatigue strength categories to this value. In one case, $3 \cdot 10^6$ stress cycles were applied due to the availability of the machine. A value of $R = 0.1$ was selected because this is relevant in practice for a lightweight structure with a large variable action and for comparison with results from the literature. However, the investigated stress ratio $R = 0.1$ does not cover the range of stress ratios in the design approach given in the FV Draft of FprEN 1995-1-1 (*CEN,* 2025), i.e. $-1 \leq R \leq 1$.

The temperature T in the bond lines, the machine stroke and the force F were measured continuously. Monitoring the temperature in the bond lines was important to ensure that the fatigue loading would not lead to an impermissible heating of the adhesive and thus to an influence on the load-bearing behaviour of the BiR.

Table 6. Loading parameters for the fatigue tests.

Parameter	Symbol	Series A1	Series A3	Series C2	Series D2
Number of fatigue tests	n	3	4	4	4
Minimum force	F_{min}	10 kN	10 kN [1)]	9 kN	7.2 kN [5)]
Mean force	F_m	55 kN	55 kN [2)]	49.5 kN	39.6 kN [6)]
Maximum force	F_{max}	100 kN	100 kN [3)]	90 kN	72 kN [7)]
Force amplitude	F_a	± 45 kN	± 45 kN [4)]	± 40.5 kN	± 32.4 kN [8)]
Stress ratio	$R = F_{min}/F_{max}$	0.1	0.1	0.1	0.1
Frequency	f	5 – 12 Hz	4 – 6 Hz	5.5 – 7 Hz	4 – 6.25 Hz
Wave shape	–	Sinus	Sinus	Sinus	Sinus
Control	–	Force	Force	Force	Force

Parameters for test on specimen A3-04: [1)] 14 kN [2)] 77 kN [3)] 140 kN [4)] ± 63 kN
Parameters for test on specimen D2-01: [5)] 9 kN [6)] 49.5 kN [7)] 90 kN [8)] ± 40.5 kN

In the fatigue test on specimen D2-01, cracks appeared after only 135'000 stress cycles, and it was suspected that these were initiated by the drying of the specimen. Therefore, it was decided to cover the end faces of the specimens with plastic tape for the remaining fatigue tests on specimens of series D2 in order to prevent excessive or too rapid drying out.

2.6 Experiments with static loading

The experiments with static loading were performed according to EN 26891 (*CEN,* 1991) including 1 cycle in the elastic range. At n'H, loading in pull-pull configuration was applied via hollow plunger hydraulic cylinders, operated by means of a hand pump. The load was increased incrementally, with the cylinder force (oil pressure) and the measured displacements being noted for each load step. In all static tests, the differential displacements at the BiR connections and some displacements in the timber member were measured. For parallel to grain specimens, the static MOE of the timber was determined in the central part of the member based on the deformation over a measuring length of 300 mm (*Steiger and Zumbrunn-Maurer,* 2024).

2.6.1 Proof loading and preloading prior to the fatigue tests

Static tensile proof loading and preloading was carried out on all specimens to assess their stiffness. For series A1, B, C1 and C2, the proof loading was done some days after production. The specimens of the series with elevated MC were proof loaded after conditioning. For series A2 and A3, around 166 days passed after the bonding process. Series D1 and D2 were loaded after 201 days. Proof loading ensured that no specimens were included in the fatigue tests that did not meet the quality requirements. Prior to the fatigue test, a static preloading in 5 identical cycles in pull-pull configuration was carried out on all specimens with a force level that corresponded to the maximum load of the fatigue tests F_{max}. The loading rate for the static experiments at Empa varied between 0.66 kN/s and 3 kN/s.

2.6.2 Pull-out tests after passing of fatigue tests

After the fatigue tests, static loading tests were carried out to determine the residual resistance and the residual stiffness of the BiR connections. The loading was force-controlled until reaching 1.75 times the maximum force of the fatigue tests F_{max}. Beyond, the loading was displacement-controlled with a rate of 0.012 mm/s for series A3 and 0.005 mm/s for series C2 and D2.

2.7 Investigations after testing

After completion of all tests, every specimen was disassembled and analysed in detail to identify the types of failure. Pictures of these investigations are presented in the research report (*Steiger and Zumbrunn-Maurer,* 2024).

3 Results and discussion

3.1 Temperatures in the bond lines during the fatigue tests

When testing specimen A1-01 under fatigue loading with a frequency of 12 Hz, the temperatures in the bond lines after 20'000 stress cycles (i.e. after 0.5 h of testing) reached 45 °C, and there was no indication that they would tend to increase less pronounced when continuing the test (*Maurer et al.,* 2022). Trials with lower frequencies revealed that with frequencies of 5 – 8 Hz, the temperatures in the bond lines could be kept in reasonable ranges regarding the mechanical performance of the epoxy adhesive at elevated temperatures (*Verdet et al.,* 2016). This was confirmed later when specimens of series A3 were tested with frequencies of 5 Hz and 6 Hz (Figure 5).

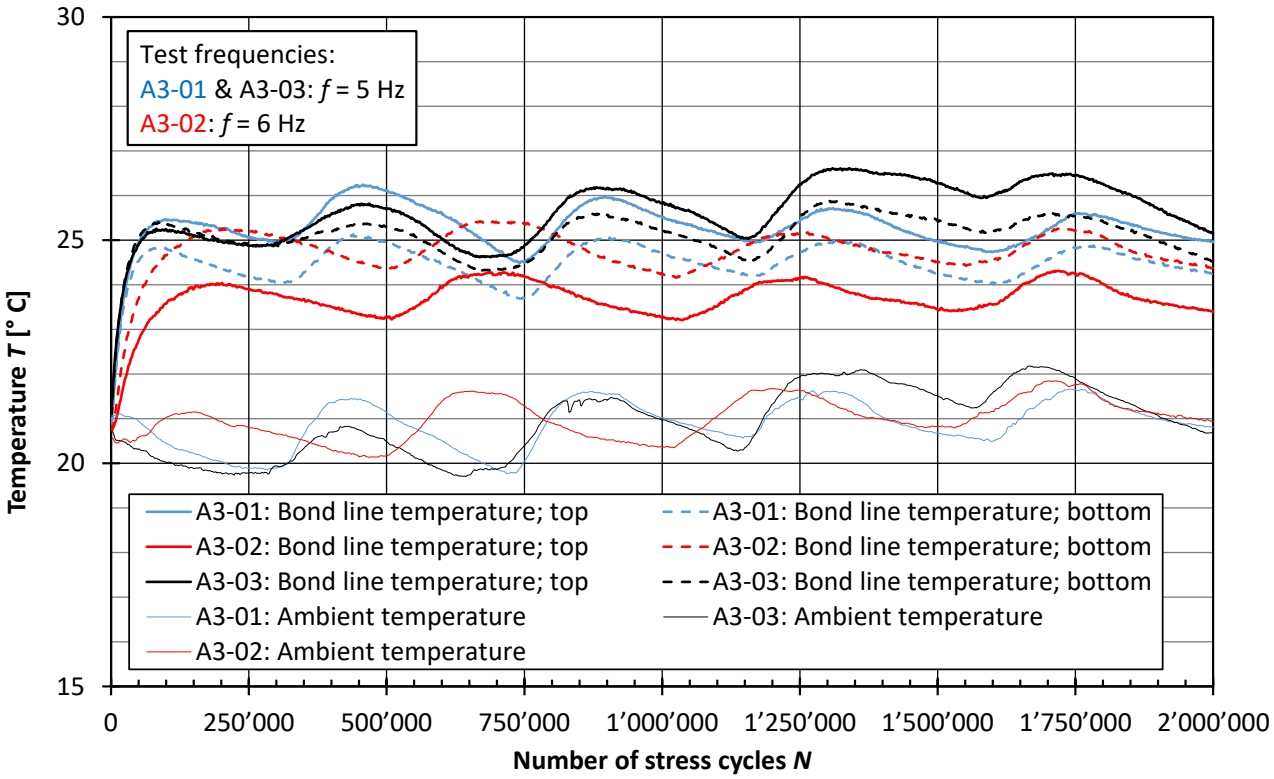

Figure 5. Development of the temperatures in the bond lines in the fatigue tests with different frequencies (BiR M16 inserted ‖ to grain in European ash GLT, 3 specimens from series A3).

3.2 BiR inserted parallel to grain in European ash GLT

The results of the tests on specimens made of European ash GLT with BiR ‖ to grain (group A) are summarized below, i.e. results of the fatigue tests (Table 7), stiffness of the BiR connections before and after fatigue loading (Table 8) and results of the pull-out tests with and without prior fatigue loading (Table 9).

In dry condition ($\omega \approx 9$ %) as well as at elevated MC ($\omega \approx 20$ %), 3 specimens passed $2 \cdot 10^6$ stress cycles (100 kN / 10 kN) without failure (Table 7). Increasing the maximum force in the fatigue test by 40 % (i.e. to the design level), led to steel failure in one of the rods after 56'000 stress cycles. The temperatures in the bond lines remain below

50 °C, if the test frequency is not higher than 6 Hz and if the chosen level of fatigue loading is in the SLS range.

Table 7. Characteristic data of the fatigue tests on the specimens with BiR inserted parallel to grain in European ash GLT (series A1 and A3).

Series A1 ($\omega \approx 9$ %)					
Specimen	Stress cycles	$\Delta\sigma_s$ [Nmm^2]	τ_{max} [N/mm^2]	Frequency [Hz]	Max. Temperature [°C] [1)]
# 1	2'054'712	287	3.4	6 – 12	55.7
# 2	2'010'000	287	3.4	8	54.2
# 3	2'010'000	287	3.4	5	48.0
Series A3 ($\omega \approx 20$ %)					
Specimen	Stress cycles	$\Delta\sigma_s$ [Nmm^2]	τ_{max} [N/mm^2]	Frequency [Hz]	Max. Temperature [°C] [1)]
# 1	2'000'486	287	3.4	5	26.2
# 2	2'000'483	287	3.4	6	25.4
# 3	2'000'486	287	3.4	5	26.6
# 4	56'175	401	4.8	5	(36.5)

[1)] Temperature in the bond line.

$\Delta\sigma_s$ Stress difference in the rods (2 GSA M16, A_s = 157 mm²).

τ_{max} Shear stress in the bond line under maximum force F_{max} (in relation to the nominal diameter of the rod and the withdrawal length).

Table 8. Connection stiffness [kN/mm] (top joint / bottom joint, respectively) determined on the specimens with BiR inserted parallel to grain in European ash GLT (group A).

Specimen	**Series A1**	**Series A2**	**Series A3**		
	K_{Proof} [1)]	$K_{Pull\text{-}out}$ [2)]	K_{Proof} [1)]	K_{Pre} [2)]	$K_{Pull\text{-}out}$ [2)]
	$\omega \approx 9$ %	$\omega \approx 20$ %	$\omega \approx 20$ %		$\omega \approx 17$ %
# 1, top	343	245	304	314	342
# 1, bottom	353	313	320	310	323
# 2, top	339	276	310	309	384
# 2, bottom	336	235	310	315	364
# 3, top	355	270	309	315	333
# 3, bottom	356	252	302	352	370
# 4, top	344	265	327	321	–
# 4, bottom	343	249	302	324	–
# 5, top	347	–	–	–	–
# 5, bottom	331	–	–	–	–
Mean value	**345**	**263**	**311**	**320**	**353**
CoV	2 %	9 %	3 %	4 %	7 %
K_{ax}	281	229	266	266	266
Deviation [3)]	+23 %	+15 %	+17 %	+20 %	+33 %

[1)] Connection stiffness determined during proof loading by neue Holzbau AG.

[2)] Connection stiffness determined in experiments at Empa with static preloading before the fatigue test or in pull-out tests after fatigue loading.

[3)] Relative difference of the mean value compared to K_{ax} according to the FV draft of FprEN 1995-1-1.

The comparison of connection stiffness in dry condition and at elevated MC (mean values 345 and 311 N/mm^2 in Table 8) shows a reduction of 10 % due to increased MC. Hence, for the design of a BiR connection in members with elevated MC, a reduction factor for the stiffness of η_ω = 0.9, as specified in the standard SIA 265 (*SIA,* 2021), should be applied. The 10 % increase in stiffness between preloading and pull-out test after fatigue loading (mean values 353 and 320 N/mm^2 in Table 8) is partly attributed to the decrease in MC (from around 20 % to around 17 %) and possibly to the post-curing of the adhesive during the fatigue test. Detailing of the specimens aimed at a ductile failure mode, i.e. for yielding of the rods, which is the desired failure mode in practice, and which represents the maximal performance regarding the resistance of groups of multiple BiR. However, the diameter in the constriction zone was kept larger than it would be designed in practice to prevent steel failure in the fatigue test. This was also the failure mode experienced in the static experiments (Table 9) and hence, the influence of MC on the load-bearing resistance cannot be quantified. From the experiments in Series A3, it can be concluded that exposing the BiR ∥ to grain in ash glulam to fatigue loading with 2·10^6 stress cycles and a bond line stress τ_{max} 3.4 N/mm² did not lead to a reduction of the withdrawal resistance, neither in dry condition (series A1, (*Maurer et al.,* 2022), nor at elevated MC (series A3). The differences in withdrawal resistance without and with prior fatigue loading (series A2 vs. A3) can be explained with the different steel quality of the rods, see 2.3.2.

Table 9. Withdrawal resistance [kN] and failure mode determined on the specimens with BiR inserted parallel to grain in European ash GLT (group A).

Specimen	Series A2	Series A3
	$\omega \approx 20$ %	$\omega \approx 17$ %
# 1	248	270
# 2	249	270
# 3	250	268
# 4	250	–
Mean value	**249**	**269**
Failure mode	**Rod yielding**	**Rod yielding**

3.3 BiR inserted perpendicular to grain in Norway spruce GLT

The results of the tests on Norway spruce GLT specimens with BiR ⊥ to grain (groups C & D) are reported below, i.e. for the fatigue tests (Table 10), the stiffness of the connections with 3 GSA M16 before and after fatigue loading (Table 11), and for the pull-out tests with and without prior fatigue loading (Table 12). In dry conditions (series C2), 3 specimens could be subjected to fatigue loading with 2·10^6 stress cycles at serviceability level (90 kN / 9 kN) without failure (Table 10). One specimen even passed 3·10^6 stress cycles (90 kN / 9 kN) without failure. Regarding temperatures, the tests confirmed the findings of the group A. With frequencies in the range of 4 – 7 Hz, bond lines of these series could be kept below 40 °C.

Table 10. Characteristic data of the fatigue tests on the specimens with BiR inserted perpendicular to grain in Norway spruce GLT (series C2 and D2).

Series C2 ($\omega \approx 9$ %)					
Specimen	Stress cycles	$\Delta\sigma_s$ [Nmm^2]	τ_{max} [N/mm^2]	Frequency [Hz]	Max. Temperature [°C] [1)]
# 1	2'034'359	172	2.1	5.5	32.9
# 2	1'999'998	172	2.1	5.9	30.6
# 3	1'998'521	172	2.1	6.5	31.3
# 4	2'999'801	172	2.1	7	32.1
Series D2 ($\omega \approx 20$ %)					
Specimen	Stress cycles	$\Delta\sigma_s$ [Nmm^2]	τ_{max} [N/mm^2]	Frequency [Hz]	Max. Temperature [°C] [1)]
# 1	422'834	172	2.1	6.25	(46.1)
# 2	2'000'500	138	1.6	5	30.5
# 3	2'000'500	138	1.6	5.9	33.8
# 4	2'000'500	138	1.6	4	37.6

[1)] Temperature in the bond line.

$\Delta\sigma_s$ Stress difference in the rods of the top joint (3 GSA M16, A_s = 157 mm²).

τ_{max} Shear stress in the bond line under maximum force F_{max} (in relation to the nominal diameter of the rod and the withdrawal length).

When in series D2 subjecting the same connections to fatigue loading at elevated MC with the same force parameters, fatigue failure in the wood (rolling shear) occurred after $0.4 \cdot 10^6$ stress cycles and the temperatures in the bond lines peaked to almost 50 °C. After having reduced the forces by 20 % (72 kN / 7.2 kN), 3 specimens passed $2 \cdot 10^6$ stress cycles without failure and the temperatures in the bond lines remained below 40 °C. It can be concluded that for the design of a BiR connection at elevated MC, for the strength, a reduction factor of $\eta_\omega = 0.8$, as specified in the standard SIA 265 (SIA, 2021), should be applied.

Concerning the connection stiffness (Table 11), only the values in cells shaded in grey should be compared directly, due to the displacement measurements not having been performed with the same equipment and precision. Looking at the limited number of available values, conclusions must be drawn carefully. The displacement measurements at the bottom joints were influenced by different steel parts with different nuts, depending on the series and different reference points depending on the test lab. A detailed evaluation of these results was not done yet. Therefore, no results are presented here, while the raw values could be found in the research report.

In series C2, tested in dry condition (MC ≈ 9 %), the stiffness of the top joints increased by 4 % for specimen C2-02 and decreased by 13 % for specimen C2-03, which is an indication that the fatigue loading with $2 \cdot 10^6$ stress cycles at serviceability level (90 kN / 9 kN) led to a slight reduction of the stiffness. After fatigue loading with $3 \cdot 10^6$ stress cycles, an 18 % lower stiffness was measured for specimen C2-04.

Table 11. Connection stiffness [kN/mm] determined on the specimens with BiR inserted perpendicular to grain in Norway spruce GLT (groups B, C and D) at the top joint (3 GSA M16).

Specimen	*Group B* and Series C1		Series C2		Series D1		Series D2	
	$K_{Pull-Out}$	K_{Proof}	K_{Pre}	$K_{Pull-Out}$	$K_{Pull-Out}$	K_{Proof}	K_{Pre}	$K_{Pull-Out}$
	$\omega \approx 9$ %		$\omega \approx 9$ %		$\omega \approx 20$ %	$\omega \approx 20$ %		$\omega \approx 18$ %
Testing @	n'H	n'H	Empa	Empa	n'H	n'H	Empa	Empa
# 1	*213* [1]	262	– [2]	201	188	202	212	–
# 2	*246*	264	254	263	201	188	195	46 [4]
# 3	*269*	279	256	224	212	199	182	138
# 4	250	230	210	173 [3]	–	204	185	117
# 5	263	–	–	–	–	187	–	–
# 6	274	–	–	–	–	203	–	–
Mean value	**260**		**240**	**229**	**198**		**194**	**128**
CoV	6 %		11 %	14 %	4 %		7 %	–
K_{ax}	305		310	310	299		299	299
Deviation [5]	-15 %		-23 %	-26 %	-34 %		-35 %	-57 %

[1] Value was not considered when calculating the mean value because a different reference point had been selected for measuring the joint deformation than for the other tests.

[2] Differential displacements at the BiR connections were not measured.

[3] Value was not considered when calculating the mean value because the specimen was tested after $3 \cdot 10^6$ stress cycles, whereas the other ones had been tested after $2 \cdot 10^6$ stress cycles.

[4] Although the specimen achieved $2 \cdot 10^6$ stress cycles in the fatigue test, damage appears to have occurred because of the fatigue stress. This value was not considered when calculating the mean value of joint stiffness.

[5] Relative difference of the mean value compared to K_{ax} according to the FV draft of FprEN 1995-1-1.

A clearer picture emerged from series D2 (i.e. specimens with elevated MC ≈ 18 %, tested with reduced forces 72 kN / 7.2 kN). The stiffness of specimen D2-02 after the fatigue test was 76 % lower than during preloading and the deformation at 72 kN reached almost 1.6 mm. Accounting for this and looking at the strongly reduced withdrawal resistance (37 %) of 117 kN (Table 12), it could be concluded that this specimen had suffered significant damage during the fatigue test. The BiR connections of specimens D2-03 and D2-04 were markedly less stiff after fatigue loading (24 % reduction in stiffness for specimen D2-03 and 37 % for specimen D2-04). The mean value of the stiffnesses of these two specimens (128 kN/mm) is 51 % lower than the mean value without fatigue loading in dry state (260 kN/mm).

The mean value of withdrawal resistance after fatigue loading at elevated MC (specimens D2-03 and D2-04) was 166 kN. Compared to the 5 static tensile tests in the same condition regarding MC (series D1 and specimens D2-05, D2-06), this corresponds to a reduction of 11 %. Compared to the mean value of the specimens tested in dry condition (Series B and C1), the reduction is 18 %. Hence, 20 % reduction for the strength at elevated MC ($\eta_\omega = 0.8$, as specified in the standard SIA 265 (*SIA,* 2021)) is recommended for design. Clause 10.2(4) of the FV Draft of FprEN 1995-1-1

(*CEN,* 2025) specifies that "For the calculation of the fatigue strength in SC 3, the characteristic strength f_k in Formula (10.2) should be multiplied by 2/3" and that "For connections the clause should be applied analogously."

In dry condition (series C2, MC ≈ 9%), the first 3 specimens did not show any reduction in withdrawal resistances after having been subjected to $2 \cdot 10^6$ stress cycles at serviceability level (90 kN / 9 kN). After $3 \cdot 10^6$ stress cycles, the withdrawal resistance of specimen C2-04 was 17 % lower than the mean value of the specimens in series B and C1. For the design of structures with more than $2 \cdot 10^6$ stress cycles, the fatigue strength should be confirmed with additional experiments.

For all specimens (i.e. with and without prior fatigue loading), the governing failure mode was rolling shear failure in the wood close to the BiR rows, with simultaneous cracking. Hence, this type of failure must be verified accordingly, when designing such a connection. However, despite respective research is available (e.g. (*Blass et al.,* 2019; *Meyer,* 2020)), there are no design rules available in the FV Draft of FprEN 1995-1-1 (*CEN,* 2025). There, Clause 11.6.1(7) simply states that "In addition to the splitting resistance …. for connections with more than two axially loaded fasteners in a row parallel to grain ($n_0 > 2$), the rolling shear failure should be verified along the perimeter of the group of fasteners".

Table 12. Withdrawal resistance [kN] and failure mode determined on the specimens with BiR inserted perpendicular to grain in Norway spruce GLT (groups B, C and D).

Specimen	*Group B* and Series C1	Series C2	Series *D1* and D2	Series D2
	$\omega \approx 9$ %	$\omega \approx 9$ %	$\omega \approx 20$ %	$\omega \approx 18$ %
Testing @	n'H	Empa	*n'H* / Empa	Empa
# 1	*210*	186	*200*	–
# 2	*211*	203	*179*	117 [1)]
# 3	*185*	204	*207*	181
# 4	209	167 [2)]	–	150
# 5	190	–	185	–
# 6	200	–	164	–
Mean value	**201**	**198**	**187**	**166**
Failure mode	**Rolling shear failure after formation of cracks**			

[1)] The specimen passed $2 \cdot 10^6$ stress cycles in the fatigue test. It seems that damage had occurred because of the fatigue stress. This value was not considered when calculating the mean value of withdrawal resistance.

[2)] Value not considered when calculating the mean value because the specimen was tested after having been subjected to fatigue loading with $3 \cdot 10^6$ stress cycles.

3.4 Design approach in the FV draft of FprEN 1995-1-1

In Figure 6 and Figure 7, the test results are compared with the SN-curves (Wöhler-curves) according to the FV draft of FprEN 1995-1-1. For the tested configuration and *R*°=°0.1, the design model leads to conservative numbers of stress cycles for the chosen levels of fatigue loading F_{max}.

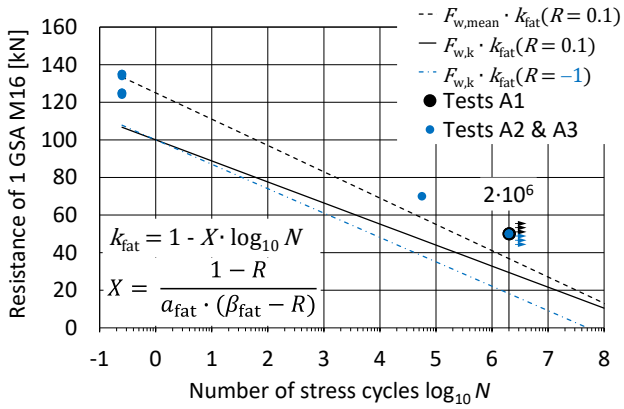

Figure 6. Experimental results of BiR ∥ to grain compared to the design model in the FV draft of FprEN 1995-1-1.

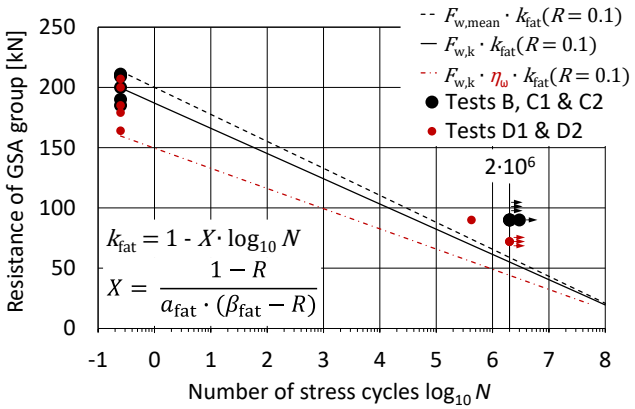

Figure 7. Experimental results of BiR ⊥ to grain compared to the design model in the FV draft of FprEN 1995-1-1.

According to the SN-curve for R = -1 (red line in Figure 6), a GSA BiR might be subjected to $2 \cdot 10^6$ fully reversed stress cycles of ±18.2 kN. The tested force amplitude of ±45 kN in the tension-tension stress range supports the expectation that the design model is conservative also for this stress ratio. However, evidence should be provided by experiments. In Figure 7, the blue SN-curve shows the proposed reduction factor for elevated MC η_ω = 0.8. This and the following proposals assume that the partial safety factor for fatigue strength is set to $\gamma_{R,fat}$ = 1.0 by the National Annexes.

4 Conclusions

From the investigations on BiR ∥ to grain in European ash GLT and BiR ⊥ to grain in Norway spruce GLT, consisting of static tests and fatigue loading with forces at SLS level and an R value of 0.1, the following conclusions can be drawn:

- The applied methodology, test setups and materialisation of specimens proved to work well for the investigation of fatigue strength of BiR at different levels of MC.
- BiR can be applied in connections subjected to fatigue loading in environment with elevated MC (e.g. to construct road bridges), provided the materials and shapes of the steel parts (rods, adapters) are optimized for fatigue loading.
- When applying high-performance BiR connections ($f_{w,k}$ > 4 N/mm²) in GLT at elevated MC (upper range of SC 2), the withdrawal resistance (for fatigue and quasi-static loading) should be reduced by 20 % in the design if the characteristic value is based on short term tests in dry conditions. This reduction would be in line with the strength reduction factor of 2/3 specified in the FV draft of FprEN 1995-1-1, Clause 10.2(4) for applications in SC 3.
- The values for the coefficients a_{fat} and β_{fat} for axially loaded BiR given in the FV draft of FprEN 1995-1-1 are considered reasonable considering the current knowledge. More tests should be performed to justify less conservative values.

- Criteria regarding the displacement increase during the fatigue test and/or regarding the residual withdrawal resistance should be defined in the standards.
- The axial slip modulus for BiR (ε = 0°) given in the FV draft of FprEN 1995-1-1 underestimates the stiffness of the tested BiR ∥ to grain configuration. For BiR ⊥ to grain with the chosen reference point on the member, the stiffness is overestimated. Assuming the reference point to be standardised and formulae for the axial slip modulus in SC 1 to be improved, the connection stiffness should be reduced by 10 % in the design for quasi-static loading at elevated MC. Stiffness reduction factors up to 0.5 should be discussed for the design of axially loaded fasteners under fatigue loading at elevated MC.
- When performing fatigue tests of BiR inserted in timber, the temperatures in the bond lines should be monitored to prevent their excessive warming. With ambient temperatures below 22 °C, test frequencies up to 6 Hz led to temperatures in the bond lines of not more than 40 °C. Respecting this limit should prevent inadmissible post-curing of the adhesives. Post-curing can lead to a beneficial behaviour of the adhesive not representing the situation in practice, where much lower frequencies of cyclic loading by vehicles occur.
- The tests on BiR ∥ to grain in European ash GLT showed that static ductility (rod yielding) can be achieved with a dedicated design, detailing and execution. Neither the fatigue loading nor the elevated MC led to questioning the provision in the FV draft of FprEN 1995-1-1, Clause 11.10.5.1(3) about ductile prior to brittle failure.
- For the specimens with BiR ⊥ to grain in Norway spruce GLT, rolling shear in the wood close to the rod rows was the governing failure mode. This was identified in the pull-out tests, for specimens with and without prior fatigue loading. Even though a respective hint can be found in the FV draft of FprEN 1995-1-1, no respective design formula is given in the standard.
- Conditioning of timber specimens to an MC to be expected in SC 2 / SC 3 takes approximately 200 days depending on the size of the specimens. Conditioning proofed to work well in a box with saturated potassium chloride (KCl) water solution and ventilation of the air in the box.
- The weighing of reference specimens with representative cross-sections showed the slower moisture uptake of lager dimensions. Their mass constancy was clearly lower than predicted by the formula for the calculated EMC. The reason for this is very likely a permanent moisture gradient which seems to establish in a timber member with dimensions as occurring in building practice.

Overall, it can be concluded that the investigation contributes to the future standardisation of fatigue and static tests on timber connections. When designing (BiR) connections for applications with elevated MC, the stiffness, withdrawal resistance and fatigue strength should be reduced. The values of the reduction factors must be aligned with the base values chosen in the standard. If a force introduced by rows of

axially loaded fasteners causes rolling shear stresses in the wood, this should be verified and hence, a suitable design approach should be added to FprEN 1995-1-1.

5 References

Arnold, M., Ehrhart, T., Lehmann, M., Strahm, T. (2021). Richtlinie zur Herstellung von verklebten Produkten aus Laubholz. Holzindustrie Schweiz, Fachgruppe Leimholz, Bern, Schweiz.

Bengtsson, C., Johansson, C.-J. (2002). GIROD – Glued-in rods for timber structures. SP Report 2002:26. Boras, Sweden.

Bernasconi, A., Ehrhart, T., Eschmann, M., Franke, S., Jockwer, R., Klippel, M., Lehmann, M., Maurer, B., Pauli, B., Ratsch, G., Schmid, H., Selter, W., Strahm, T. (2021). Verklebte Laubholzprodukte für den statischen Einsatz. Lignum – Holzwirtschaft Schweiz, Zürich.

Blass, H. J., Flaig, M., Meyer, N. (2019). Row shear and block shear failure of connections with axially loaded screws. INTER Meeting Fifty-Two. Online. Paper INTER/52-7-6:

Bletz-Mühldorfer, O., Diehl, F., Bathon, L., Myslicki, S., Walther, F., Grunwald, C., Vallée, T. (2018). Ermüdungsverhalten von eingeklebten Stäben. Bauen mit Holz 5, 30 - 35.

EN 338 (2016). Structural timber - Strength classes. CEN, Brussels, Belgium.

EN 1995-1-1 (2004). Design of timber structures, Part 1-1: General - Common rules and rules for buildings. CEN, Brussels, Belgium.EN 1995-2 (2004) Design of timber structures, Part 2: Bridges. CEN, Brussels, Belgium.

EN 1995-2 (2004) Design of timber structures, Part 2: Bridges. CEN, Brussels, Belgium.

EN 17334 (2021). Glued-in rods in glued structural timber products - Testing, requirements and bond shear strength classification. CEN, Brussels, Belgium.

EN 26891 (1991). Timber structures – Joints made with mechanical fasteners: General principles for the determination of strength and deformation characteristics. CEN, Brussels, Belgium.

FprEN 1995-1-1 (2025). Design of timber structures, Part 1-1: General – Common rules and rules for buildings. Formal Vote Draft. Doc. CEN/TC 250/SC 5/N2259. CEN, Brussels, Belgium.

Erchinger, C., Steurer, A. (2005). In Holz eingeleimte Gewindestangen – Ermüdungsverhalten. Bulletin Holzforschung Schweiz, 13(1), 12 - 13.

ETA-19/0752 (2020). Timber Structures – Glued-in rods for timber connections (GSA-Technology). EOTA, Brussels, Belgium.

Gehri, E. (2000). Klassische Verbindungen neu betrachtet. 17. Dreiländer Holztagung "Holz: Architecture - Research - Technology". Luzern, Schweiz. 43 - 50.

Maurer, B., Gehri, E., Strahm, T., Steiger, R., Affolter, C. (2022). Fatigue strength of axially loaded steel rods bonded in European ash glulam. 4th International Conference on Timber Bridges ICTB. Biel/Bienne, Switzerland.

Meyer, N. (2020). Tragfähigkeit mechanischer und geklebter Verbindungsmittel in Buchenfurnierschichtholz. PhD Thesis. Karlsruher Institut für Technologie (KIT), Karlsruhe, Germany.

Molina, J. C., Calil, C., Carreira, M. R. (2009). Pullout strength of axially loaded steel rods bonded in glulam at a 45 degrees angle to the grain. Materials Research-Ibero-American Journal of Materials, 12(4), 427 - 432.

Myslicki, S., Bletz-Mühldorfer, O., Diehl, F., Lavarec, C., Vallée, T., Scholz, R., Walther, F. (2019). Fatigue of glued-in rods in engineered hardwood products - Part I: Experimental results. Journal of Adhesion, 95(5-7), 675-701.

Myslicki, S., Walther, F., Bletz-Mühldorfer, O., Diehl, F., Lavarec, C., Beber, V. C., Vallée, T. (2019). Fatigue of glued-in rods in engineered hardwood products – Part II: Numerical modelling. Journal of Adhesion, 95(5-7), 702 - 722.

Norm SIA 265 Holzbau (2021). Schweizerischer Ingenieur- und Architektenverein SIA, Zürich, Schweiz.

Reichel, S. (2015). Modellierung und Simulation hygro-mechanisch beanspruchter Strukturen aus Holz im Kurz- und Langzeitbereich. PhD Thesis. Technische Universität Dresden, Germany.

Steiger, R., Serrano, E., Stepinac, M., Rajcic, V., O'Neill, C., McPolin, D., Widmann, R. (2015). Strengthening of timber structures with glued-in rods. Construction and Building Materials, 97, 90 - 105.

Steiger, R., Zumbrunn-Maurer, B. (2024). Bericht zum Projekt WHFF-CH 2022-10: Ermüdungsverhalten von in BSH eingeklebten Gewindestangen mit Einsatz im Brückenbau. https://www.aramis.admin.ch/Texte/?ProjectID=57787

Tlustochowicz, G., Serrano, E., Steiger, R. (2010). State-of-the-art review on timber connections with glued-in steel rods. Materials and Structures, 44(5), 997 - 1020.

Verdet, M., Salenikovich, A., Cointe, A., Coureau, J. L., Galimard, P., Toro, W. M., Blanchet, P., Delisee, C. (2016). Mechanical performance of polyurethane and epoxy adhesives in connections with glued-in rods at elevated temperatures. Bioresources, 11(4), 8200 - 8214.

DISCUSSION

The paper was presented by R Steiger

S Winter asked why parallel to grain was considered in ash but perpendicular to grain was considered in spruce. R Steiger said that budget constraints led to concentrating testing on the boundary situations to seek reduction in cost. S Winter received clarification of the stress level in the bond line.

C Demirci questioned the tolerance for this type of connections if they were made on site and asked how to ensure this work in service class 3 conditions. R Steiger replied that this type of connections needs a company with good quality control. In this case the company has more than 20 years of experience. The work was not extrapolated towards service class 3.

C Sandhaas commented on the test setup of 3 or 4 bonded-in rods and asked if the number of bonded-in rods in a connection would affect the conclusions. R Steiger agreed that this could affect the results.

H Blass commented about the statement that there is lack of guidance in the code on rolling shear failure in the perpendicular to grain cases. He said Karlsruhe Institute of Technology has worked on this topic with a proposal available. R Steiger stated that they are aware of the work but the partner company has been working on their own proposal.

P Dietsch commented that the paper indicated that a reduction to 2/3 for SC3 seems to be safe. He asked if there was any data available for justification. R Steiger agreed that they do not have test results on this.

U Hübner said high risk is associated with on-site gluing and implied that on-site gluing should generally be avoided; hence, quasi-industrial, factory made systems are needed.